Modeling urban energy dynamics under clustered urban heat island effect with local-weather extended distributed adjacency blocks

5 authors, including:

Rui Ma
City University of Hong Kong
6 PUBLICATIONS **12** CITATIONS

SEE PROFILE

Bin Ren
Shanghai University
31 PUBLICATIONS **47** CITATIONS

SEE PROFILE

Dong Zhao
Michigan State University
71 PUBLICATIONS **850** CITATIONS

SEE PROFILE

Jiayu Chen
City University of Hong Kong
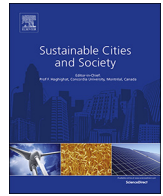**93** PUBLICATIONS **1,157** CITATIONS

SEE PROFILE

Some of the authors of this publication are also working on these related projects:

Knowledge Acquisition View project

China Rural Building Performance Design View project

Modeling urban energy dynamics under clustered urban heat island effect with local-weather extended distributed adjacency blocks

Rui Ma[a], Bin Ren[b], Dong Zhao[c], Jiayu Chen[d,*], Yujie Lu[e]

[a] Institute of Rail Transit, Tongji University, No.4800 Cao'an Road, Jiading District, Shanghai, 200092, China
[b] School of Mechatronic Engineering and Automation, Shanghai Key Laboratory of Intelligent Manufacturing and Robotics, Shanghai University, Shanghai, 200444, China
[c] School of Planning, Design and Construction, Michigan State University, 201K Human 10 Ecology Building, 552 W Circle Drive, East Lansing, MI, 48824, USA
[d] Department of Architecture and Civil Engineering, City University of Hong Kong, Y6621, AC1, Tat Chee Ave, Kowloon, Hong Kong
[e] Department of Building Engineering, College of Civil Engineering, Tongji University, No.1239 Siping Road, Yangpu District, Shanghai, 200092, China

ARTICLE INFO

ABSTRACT

Buildings are the major energy consumers in cities. To promote building energy efficiency and urban sustainability, researchers developed comprehensive digital simulation tools, such as CitySim, CityBES, and Autozoner, efforts to investigate, understand, and predict energy dynamics of urban buildings. However, different from independent buildings in rural areas, urban buildings have complicated interactions with surrounding buildings and the environment. Owing to the computational complexity of large building numbers, these models chose top-down or regression methods with universal weather conditions. However, a reliable prediction of building energy dynamics needs a comprehensive understanding of the thermal process of building physical elements, which is often weld by the bottom-up methods. Therefore, this study proposed a novel local-weather extended distributed adjacency blocks (LW-DAB) model that incorporates bottom-up distributed adjacency blocks (DAB) simulation and allows customizable local micro-climate clusters. This study also deployed a city building digital model with 1175 buildings and compared the results with the conventional typical morphological year weather-based simulation in three different climate regions. By introducing the impacts of urban island effects (UHI) based on building the morphological relationship, the results suggest that the proposed LW-DAB model not only allows independent micro-climate assignment for each building but also half the simulation time with 5% accuracy loss compared with the conventional whole city simulation model.

1. Introduction

The rapid population growth results in great demand for housing in cities and expands the boundary of the city skyline. With the changes of the ground surfaces of cities, the local urban climates are significantly affected (Xu et al., 2017). Urban heat island effect is such a result that the urban space is warmer than the rural space in the same city (Oke, 1973, 1982). Drastic local climate changes result in variation in building energy load for cooling, heating, and ventilation, especially for densely populated cities. Several recent studies reported that the cooling load of each urban building can increase from 5% to 30 %, depending on UHI intensity, amount of solar gains, and cooling setpoint (Crawley, 2008; Salvati, Coch Roura, & Cecere, 2017). In addition, UHI also results in waste heat generation and additional fossil fuel consumption (Silva, Silva, & Santos, 2018; Xu, Zhou, Wang, Xu, & Yang, 2019). Therefore, investigating the dynamics of the UHI effect in the city-scale is essential for optimizing energy management and building

sustainable cities (Mauree et al., 2019). Therefore, many researchers proposed city-scale energy simulation tools and weather-based computational methods to mimic and predict urban building energy dynamics under various climate conditions (Ali-Toudert & Böttcher, 2018; Yang, Jin, Yao, Zhu, & Peng, 2017).

City-scale energy simulation methods can be categorized as top-down methods and bottom-up methods. Top-down methods estimate building energy consumption based on the historical record or economic variables of a city building stock, while bottom-up methods estimated the building energy dynamics based on thermal physics and synthesis features of building structures (Swan & Ugursal, 2009; Torabi Moghadam et al., 2019). Top-down methods have higher computational efficiency as it relies on the interrelationships between input data features, while bottom-up methods are slow due to the computational complexity of the building thermal dynamic process among different building elements. Bottom-up methods are more suitable for energy dynamic simulation under the context of various climate conditions, as

the local temperature, radiation, and wind speed can directly impact the thermal physics of the building environment. However, existing bottom-up city-scale energy simulation methods have two major theoretical constraints. First, due to the heavy computational requirements, existing simulation methods usually require a high computational resource, long simulation time, and negligence of local climate variation (for efficiency purpose, existing simulation methods apply a uniform weather file for the whole city). Second, the inter-building effects, such as shading and reflection, are simplified to improve simulation efficiency (Pisello, Taylor, Xu, & Cotana, 2012). To fill in these research gaps, this study proposed a local-weather distributed adjacency block model to simulate the whole city model as a distributed system that is linked by local climates and inter-building effects. With the proposed model, the whole city model can be simulated iteratively and parallelly by buildings with clear physical boundary conditions.

2. Background

2.1. Urban heat island effect and inter-building effects

UHI effect is the results of the changed sky view factor, solar reflectivity, heat capacity, and roughness of the land surfaces, which is caused by increasing building density and height (Oke, 1973). Researchers proposed UHI intensity to quantify the temperature and solar differences caused by UHI. Many UHI intensity studies suggested that urban buildings with higher UHI intensity to higher external air temperatures, lower wind speeds, and lower heat loss during the night (Chan, 2011; Ignatius, Wong, & Jusuf, 2015; Kolokotroni, Giannitsaris, & Watkins, 2006; Kolokotroni & Giridharan, 2008; Stewart & Oke, 2012). Salvati et al. reported that the maximum average UHI intensity to be 2.8 °C in winter and 1.7 °C in summer and when it reaches 4.3 °C it will increase the sensible cooling load of residential buildings by around 18%–28% (Salvati et al., 2017). Yang et al. (2017) assessed the impact of the UHI and concluded it may increase the cooling load by 11.2 %–25.2 % for a commercial and a residential building. Therefore, many researchers concluded that by introducing vegetations, reflective building services, and heat storage materials can effectively remedy UHI's impact and promote building energy efficiency (Coccolo, Kämpf, Mauree, & Scartezzini, 2018; Morini, Touchaei, Castellani, Rossi, & Cotana, 2016; Touchaei & Akbari, 2015). Also, understanding the energy balance under UHI's context can guide the design of a new generation of zero UHI impact buildings (He, 2019) and sensitive building design (Dhalluin & Bozonnet, 2015).

Due to the differences in the surrounding environment of a building, UHI could have a different impact on a buildings' thermal load. At the same time, as the solar and long-wave radiation fluxes are characterized by multiple diffuse and specular reflections at the building surfaces in a street or city canyon configurations, the impacts of UHI can be complicated and interact with the building characteristics (He, Hoyano, & Asawa, 2009). With different urban morphology, such as the building height, size, orientation, density and layout, a city can have multiple local urban microclimates (UMC) given various surrounding environments (Dorer et al., 2013; Han, Taylor, & Pisello, 2017). For example, Kim, Gu, and Kim (2018) employed Urban Weather Generator (Bueno, Norford, Hidalgo, & Pigeon, 2013) to assess the UHI effect with different urban morphology and climate zones and concluded that the local climate conditions should be properly considered for sustainable building environment development. Golany concluded that among the urban morphology, the street orientation has the highest regional thermal impact (Golany, 1996). Jin, Cui, Wong, and Ignatius (2018) and Ignatius et al. (2015) concluded that the building density affects the receivable external heat gain, ambient temperature, urban ventilation, and outdoor thermal comfort. They suggested investigating the urban building energy models with more comprehensive methods with the consideration of local microclimate. In addition, the local climate also affects the interactions between adjacent buildings. Pisello et al. (2012),

Pisello, Castaldo, Taylor, and Cotana (2014) reported that the mutual shading among buildings results in a significant error in simulation and the error can be up to 42 % in summer and 22 % in winter. Mehaoued & Lartigue (2019) and Han, Taylor, and Pisello (2015) also found that the reflective glass façades and retro-reflective façades can impact the neighborhood microclimate and lead to an increase in the cooling demand. Based on these findings, it can be concluded that urban microclimate and inter-building effects have complicated interrelationships that result in errors in city-scale building energy prediction and simulation.

2.2. Energy modeling and simulation for cities

Bottom-up energy modeling methods collect the information on building materials, geometry, mechanical systems, occupants' behavior, and climate conditions to build 3D digital models and execute simulation core, such as EnergyPlus. For example, conventional building energy simulation (BES) tools apply the physical heat and mass flow theory to predict the energy demand of a building to provide decision supporting tools for the building managers or develop optimization strategies to minimize the building energy consumption (Coakley, Raftery, & Keane, 2014; Peeters, Dear, Hensen, & D'haeseleer, 2009; Wang, Chen, Hong, & Zhu, 2018; Wang, Hong, Li, Wang, & Chen, 2019). Based on this idea, researchers extend the individual building scale to a larger neighborhood-scale or city-scale models, such as CitySim (Robinson et al., 2009), Urban Modeling Interface (UMI) (Reinhart, Dogan, Jakubiec, Rakha, & Sang, 2013), City Building Energy Saver (CityBES) (Chen, Hong, & Piette, 2017), and "Autozoner" modeling strategy (Dogan, Reinhart, & Michalatos, 2016). However, due to the convective heat exchange and wind flow pattern, inter-building effects cannot be simply neglected (Dorer et al., 2013), as the local building environment is entangled with inter-building effects and requires heavy thermal physics computations. To promote higher efficiency, these simulation methods suggest uniform building configuration and climatic conditions. Some researchers proposed a more comprehensive method to generate local climate conditions. For example, Mauree et al. developed the Canopy Interface Model (CIM) to generate a high-resolution vertical profile for wind, potential temperature and humidity for specific buildings (Mauree, Blond, Kohler, & Clappier, 2017). CIM can be coupled with CitySim to improve the climatic boundary conditions used in the calculation of the energy balance (Mauree, Coccolo, Kaempf, & Scartezzini, 2017) and Perera et al. used this coupling to look at the impact of planning scenarios on the optimization of energy systems (Perera, Coccolo, Scartezzini, & Mauree, 2018). However, with the growth of the model size, it cannot be extended to large cities due to the limit of computer memory. When a city-scale model integrates thousands of buildings, it would lead to extremely long construction time and simulation run time. Therefore, this study intends to incorporate both inter-building effects and local climatic conditions and develop a distributed simulation method that is scalable, reliable, and an efficient city-scale energy simulation tool.

3. Methodology

3.1. LW-DAB model

The proposed method LW-DAB model consists of two major modules, including a local weather generation (LWG) module and a DAB simulation module. The LWG module generates microclimate weather files for building blocks while the DAB module implements a "decomposition-reconstruction" process to simplify a whole city model as a collection of "target building + boundary conditions" model based on inter-building effects. Fig. 1 shows the scheme of the proposed LW-DAB model.
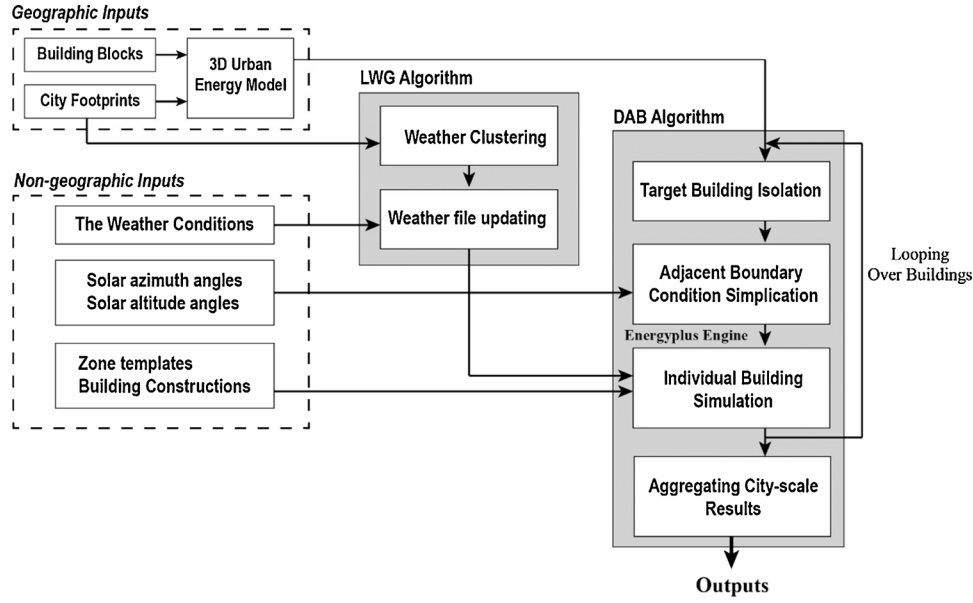
Fig. 1. The scheme of the LW-DAB model.

3.2. 3D city model construction

To simulate city-scale energy dynamics, the 3D building geometry models are necessary to identify building envelopes. This study utilized 2D building footprints and building stock information to construct the 3D model, available city dataset should in the format of GIS, CityGML, GeoJson, or IDF. 2D building footprint models consist of both the building spatial distribution information and their interrelationships (Macumber et al., 2016). With the building stock information, the footprint can be colored based on the building height, materials, and window-to-wall ratio (WWR). Then with a building thermal zoning and the heating, ventilation, and air conditioning (HVAC) system template, the 3D city model can be constructed. Fig. 2 illustrates the process of 3D city model construction for a 125-building stock.

3.3. LWG module and simulation

3.3.1. Step 1: building clustering

The core concept of simulating UHI's impact is assigning customized local weather files for buildings in different regions. It is necessary to identify the intensity of UHI for different building groups. The first step of local weather generation is clustering buildings into groups to quantify their UHI based on the Town Energy Budget (TEB) scheme (Bueno et al., 2013; Masson, 2000). The TEB scheme suggests three parameters to execute classification, including average building height (h_{bld}), vertical-to-horizontal urban area ratio (VH), and horizontal building density (ρ_{bld}).

According to TEB scheme, the first bounce of solar radiation for walls and roofs can be quantified with K_w as

$$K_w = K_{dir} \bullet \left(\frac{w_r}{h_{bld}} \bullet \left(\frac{1}{2} - \frac{\theta_0}{\pi} \right) + \frac{1}{\pi} \bullet \tan(\lambda) \bullet (1 - \cos(\theta_0)) \right) + F_w \bullet K_{dif} \quad (1)$$

where K_{dir} is the direct solar radiation; K_{dif} is the diffuse solar radiation; w_r is the average road width ($w_r = \frac{2 \bullet h_{bld} \bullet (1 - \rho_{bld})}{VH}$); λ is the solar zenith angle; θ_0 is the critical canyon orientation for which the road in no longer sunlit.

$$\theta_0 = \arcsin \left(\min \left(\frac{w_r}{h_{bld}} \bullet \frac{1}{\tan(\lambda)}, 1 \right) \right) \quad (2)$$

F_w is the wall sky view factor and can be computed with Eq. (3).

$$F_w = \frac{1}{2} \bullet \left(\frac{h_{bld}}{w_r} + 1 - \left(\left(\frac{h_{bld}}{w_r} \right)^2 + 1 \right)^{\frac{1}{2}} \right) \bullet \frac{w_r}{h_{bld}} \quad (3)$$

Solar reflections then can be calculated with Eq. (4).

$$M_w = \frac{R_w + F_w \bullet \rho_w \bullet R_r}{1 - (1 - 2 \bullet F_w) \bullet \rho_w + (1 - F_r) \bullet F_w \bullet \rho_r \bullet \rho_w} \quad (4)$$

where ρ_w represents the wall surface reflectivity and $R_w = \rho_w \bullet K_w$. Finally, the total solar radiation (S_w) received by walls is given in Eq. (5).

$$S_w = K_w + (1 - 2 \bullet F_w) \bullet M_w + F_w \bullet M_r \quad (5)$$

The above method is compatible with various clustering methods, to simplify the calculation, this study chose the classic k-mean clustering. k-mean clustering method can partition the building block data into k groups based on the parameter closeness and similarity. Based on Oke's study (Oke, 2006), this study assumed a 500 m radius clustering area, which can be monitored by one single urban weather station. The average building height (h_{bld}), vertical-to-horizontal urban area ratio (VH), and horizontal building density (ρ_{bld}) were used as the major clustering variables, they can be computed with

$$h_{bld} = \frac{\sum_{i=1}^{N} h_i}{N} \quad (6)$$

$$VH = \frac{\sum_{i=1}^{N} F_{Ai}}{A_{urb}} \quad (7)$$

$$\rho_{bld} = \frac{\sum_{i=1}^{N} F_{Ti}}{A_{urb}} \quad (8)$$

where h_i is the height of building i; F_{Ti} is the footprint of building i; F_{Ai} represents the façade area of buildings i; A_{urb} is the area of the circle defining the urban site.

3.3.2. Step 2: updating local weather file

Conventional building energy dynamic simulation utilizes typical meteorological year (TMY) weather data or actual meteorological year (AMY) weather data to calibrate and computer building energy loads (Street, Reinhart, Norford, & Ochsendorf, 2013). The LWG model utilizes and extended the urban weather generator (UWG) model (Bueno et al., 2013) to produce the "*.EPW" weather files at street levels. The UWG is a streamlined meteorological method proposed by Bueno et al.
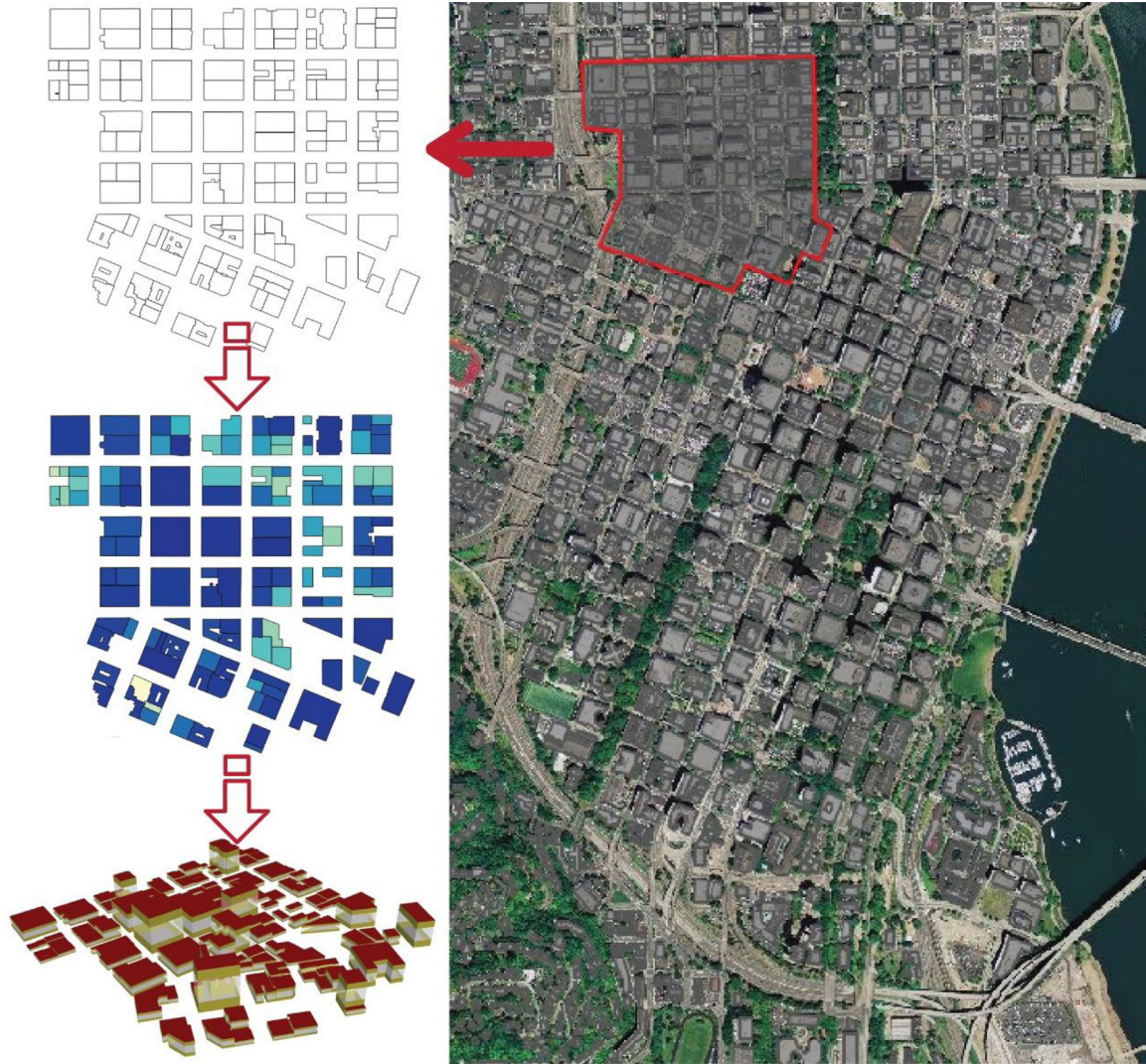
Fig. 2. The process of the 3D city model construction.

(2013) that capable of generating local weather conditions based on the urban thermal balance. It consists of four modules, including the Rural Station Model (RSM), the Vertical Diffusion Model (VDM), the Urban Boundary-Layer (UBL) model, and the Urban Canopy and Building Energy Model (UC-BEM). Fig. 3 shows the extended UWG of this study. The proposed LWG model modified the UWG model in two aspects. First, LWG applied the clustering method to divided urban buildings into several clusters based on their morphology and independently generate their weather file based on UWG. Second, in addition to temperature distribution, the LWG also modified the radiation level based on the Solar azimuth and altitude angles.

(a) The rural station model (RSM) calculates rural sensible heat fluxes (H_{rur}) based on the measured climate data. H_{rur} is computed from averaging temperature of the ground soil layers. Eqs. (9) and (10) represents the balance equation of the heat exchange in a soil layer and the first soil layer.

$$d_i \bullet (\rho c)_i \bullet \frac{\partial T_i}{\partial t} = C_{i,i+1} \bullet (T_{i+1} - T_i) + C_{i,i-1} \bullet (T_{i-1} - T_i) \tag{9}$$

$$d_1 \bullet (\rho c)_1 \bullet \frac{\partial T_1}{\partial t} = C_{1,2} \bullet (T_2 - T_1) + Q_{surf} \tag{10}$$

where d_i is the depth; $(\rho c)_i$ is the volumetric heat capacity; T_i is the average temperature of a layer; i is the index of a soil layer; Q_{surf}

represents the sum of net radiation, sensible and latent heat fluxes at the soil surface; $C_{i,j}$ is the mean thermal conductance between two layers.

(a) The vertical diffusion model (VDM) computes vertical air temperatures (θ_{rur}) profiles above the weather station. The temperature distribution can be presented as following the diffusion equation.

$$\frac{\partial \theta(z)}{\partial t} = -\frac{1}{\rho(z)} \bullet \frac{\partial}{\partial z} \left(\rho(z) \bullet K_d \bullet \frac{\partial \theta(z)}{\partial z} \right) \tag{11}$$

where θ is the potential air temperature; z is the height of a reference layer. As the reference boundary conditions, when z approximate 150 m the vertical slope of potential temperature $\frac{\partial \theta(z)}{\partial z}$ is equal to 0. Usually, the weather station measures the temperature at $z = 2$ m.

(a) The urban boundary layer model (UBL) calculates the air temperature of an urban boundary layer (T_{ubl}) above the specific urban canopy layer. The heat flow balance for a specific volume inside the urban boundary layer is

$$V_{CV} \bullet \rho \bullet c_v \bullet \frac{d\theta_{urb}}{dt} = H_{urb} + \int u_{ref} \bullet \rho \bullet c_p \bullet (\theta_{ref} - \theta_{urb}) dA_f \tag{12}$$

where V_{CV} is the control volume; c_v and c_p represent the air specific heat at constant volume and pressure; H_{urb} is the sensible heat flux at the
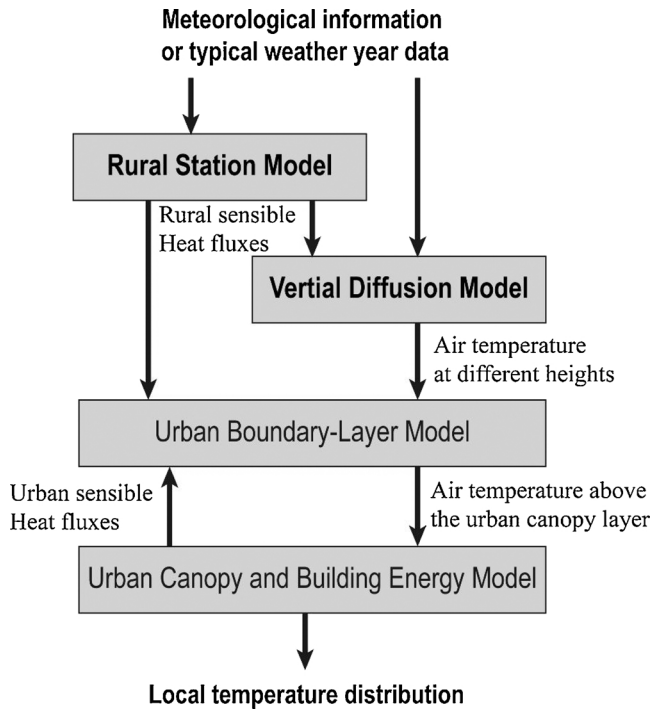
Fig. 3. The scheme of the extended UWG method.

surface of the control volume; θ_{urb} and θ_{ref} are the average potential temperature and reference potential temperature of the control volume; u_{ref} is the reference air velocity; A_f is the lateral area of heat exchange.

The value of u_{ref} depends on the advection effect driven by a geostrophic wind and the urban breeze circulation. The circulation velocity (u_{circ}) can be calculated by

$$u_{circ} = k_w \bullet \left(\beta \bullet z_i \bullet \frac{H_{urb} - H_{rur}}{\rho \bullet c_p} \right)^{1/3} \tag{13}$$

where k_w is a constant (approximate to 1); β is the buoyancy coefficient and equals to $\frac{g}{\theta}$.

(a) The urban canopy and building energy model (UC-BEM) can generate weather files that incorporate microclimate conditions and modify the generic weather files based on previous calculations. The air temperature of the urban canyon (T_{urb}) can be computed with the sensible heat exchange (between the canyon air and the atmosphere) and radiant heat exchange (between the canyon air and the sky). The surface coefficients of the Forced and buoyancy-driven air at day and night can refer to Bueno et al.'s work (Bueno et al., 2013).

The urban canyon energy balance equation if

$$V_{can} \bullet \rho \bullet c_v \bullet \frac{dT_{urb}}{dt} = A_w \bullet h_w \bullet (T_w - T_{urb}) + A_r \bullet h_r \bullet (T_r - T_{urb})$$
$$+ A_r \bullet h_{rd,sky} \bullet (T_{sky} - T_{urb}) + A_{win} \bullet U_{win} \bullet (T_{in} - T_{urb})$$
$$+ \dot{V}_{inf/vent} \bullet \rho \bullet c_p \bullet (T_{in} - T_{urb}) + u_{ex} \bullet \rho \bullet c_p \bullet (T_{ubl} - T_{urb})$$
$$+ H_{waste} + H_{other} \tag{14}$$

where V_{can} is the volume of the specific urban canyon; T_w, T_r and T_{sky} are the effective temperature of walls, roads, and the sky, respectively; T_{in} is the indoor air temperature; h_w and h_r represent the heat transfer coefficients of walls and roads; $h_{rd,sky}$ is the radiant heat transfer coefficient between the urban canyon air and the sky; U_{win} is the U-value of windows on both sides; $\dot{V}_{inf/vent}$ is the exfiltration airflow rate; u_{ex} is the exchange velocity between the in-canopy and above-canopy flows;

H_{waste} represents the wasted heat fluxes released from the HVAC system; H_{other} is other anthropogenic sources of the heat.

3.4. DAB module and simulation

The concept of the DAB algorithm intends to decompose the whole city model into a collection of independent and executable building energy simulation models (Ma, Geng, Yu, Chen, & Luo, 2019; Zheng, Chen, & Luo, 2019). Each individual building model was bounded with inter-building effects, such as shading and reflection. Then each building energy model can be simulated with a thread/process of a computer or multiple computers, the elastic feature allows flexible and efficient simulation without constraints of the computer memory. After iterative simulation of all individual building models, then the results can be aggregated back to the whole city energy dynamics. Fig. 4 illustrates how the DAB algorithm decomposes and reconstructs the individual building models. A more detailed explanation of the major steps of the DAB algorithm is shown in the following sections.

3.4.1. Step 1: target building isolation

Target building isolation refers to the decomposition of a city model into multiple individual building models. The DAB algorithm extracts detailed individual building features from the GIS database and simply adjacent buildings as shading surfaces. According to the clustering radius above, this step still takes 500 m as an optimal radius value to filter out surrounding buildings that are far away from the target building, as shown in Fig. 4. (where WWR is taken 0.5 as an example for analysis).

3.4.2. Step 2: adjacency selection

This step clarifies how to select components of the inter-building effects (IBEs), like radiant heat exchange between exterior surfaces of buildings and integration with urban microclimate, are regarded as inter-building boundary conditions that glue buildings into an interconnected city. This study incorporates three types of IBEs that are caused by adjacent buildings, including mutual shading, mutual reflection, and microclimate. As the nature of building materials is fixed and microclimate has been considered in the weather file modification, this step mainly considers shading impact as boundary conditions to remove irrelevant adjacent buildings.

The adjacency selection is composed of two parts, solar angle selection, and shading plane selection. As buildings that have mutual shading and reflection with the target building are only nearby ones, the aim is to remove irrelevant buildings that cannot generate shadings and further simplify the individual building model in Step1. Firstly, in the solar angle selection, we take shadows as the connection of the collaborative response of energy consumption between buildings. Due to that the shadow direction and length of each shading building are related to solar azimuth and altitude angles in a year, respectively, this study proposes to utilize these angles to compute, every hour, the shadow planes and eliminate the adjacent buildings, as shown in Fig. 6(b). Secondly, in the shading plane selection, redundant shading buildings whose shadows cannot reach the target building are further deleted. The buildings within the shading plane and on the direction of the solar path (the direction of sunrise and sunset) will be screened out. The final shading buildings are determined by comparing the height of near shading buildings with the shadow height of distant shading buildings. For a specific city, solar azimuth and altitude angles are periodically changed every year, the simplified model can finally downscale to a model with detailed target building with few shading surfaces, as shown in Fig. 6(c), even further study can store these relevant shading buildings and subsequently extract them from the city database without repeating the adjacency selection.

3.4.3. Step 3: individual building simulation

After the down-scaled building energy model is built, the distributed simulation can be carried out for each selected target building. It is
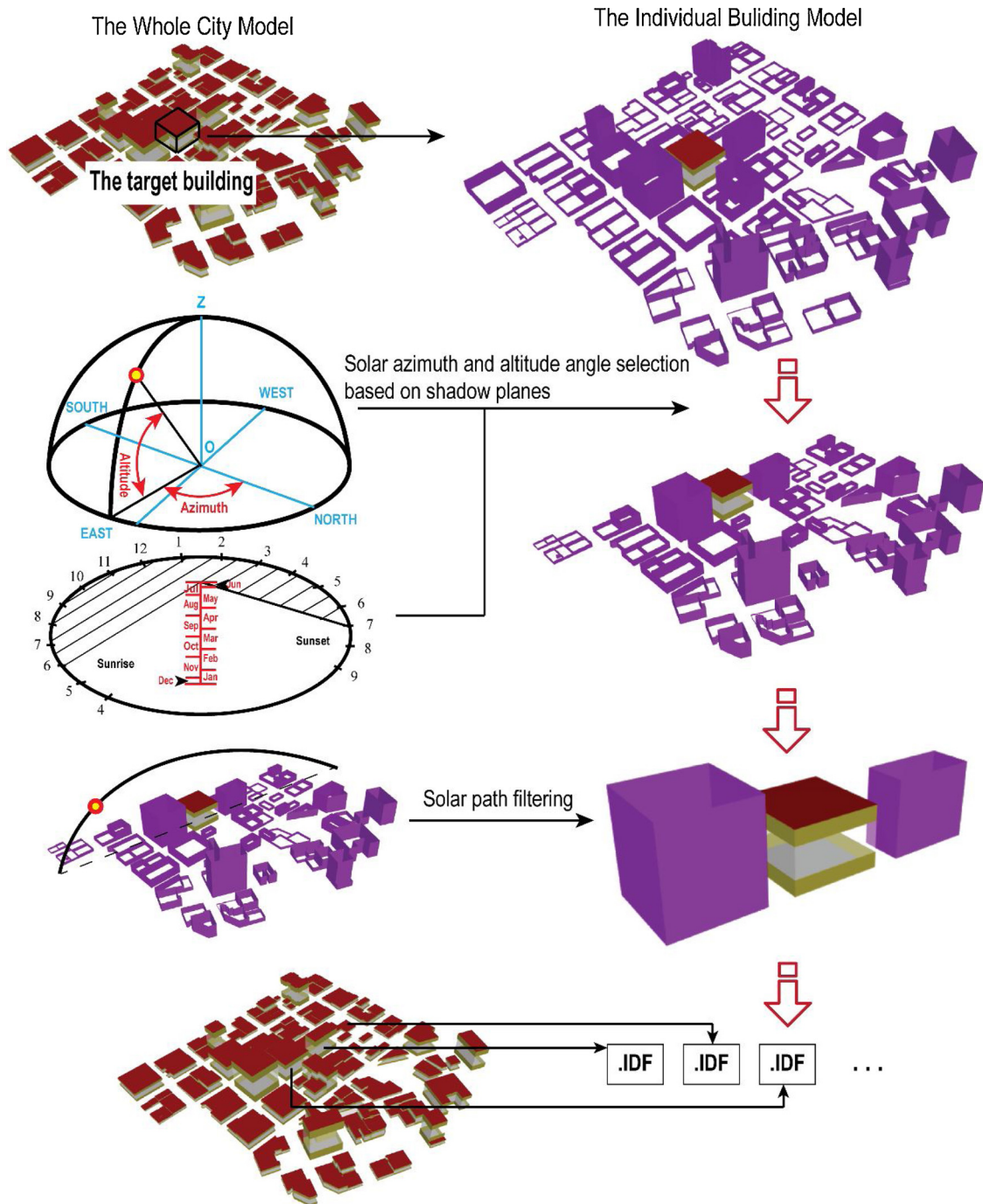
Fig. 4. The DAB algorithm process for city-scale building energy model decomposition.

noteworthy that the individual simulation should be conducted with a corresponding weather file that generated in Section 3.3. Due to that, the DAB model eliminates unnecessary components and the energy consumption can be calculated within less time. Then, all previous steps are repeated again for each individual building for the whole city. Although it might not be as accurate as detailed models due to the simplification, it still offers advantages for quick energy analysis with fewer inputs (Chen et al., 2017).

3.4.4. Step 4: aggregating city-scale simulation results

Finally, after each building is successively computed and recorded, this step will integrate all the results in the city model and finish the city-scale energy consumption.

4. Investigating clustered urban heat island effect with LW-DAB model

4.1. Comparative efficiency of the LW-DAB model

To assess the validity of the proposed LW-DAB model, this study utilized a real city dataset to conduct the energy dynamic simulation with the EnergyPlus core. To simplify the simulation model, all building utilized the same thermal zone template and same WWR as 0.5. The simulation was run on a laptop with an Intel i5 dual-core central processing unit (Intel Core i5-3427U @ 1.80 GHz), 8 GB of RAM, and a 256 G solid-state hard drive.

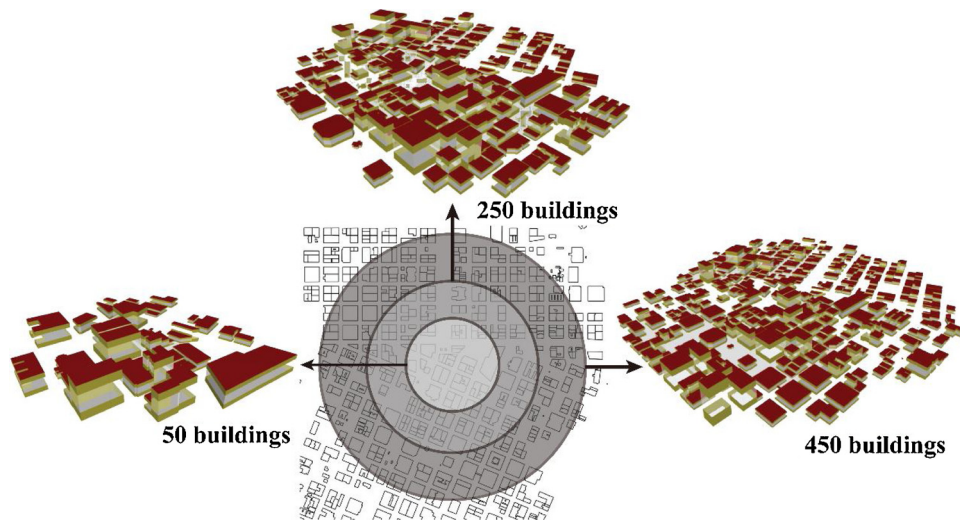The first validation test aims to examine the efficiency and accuracy

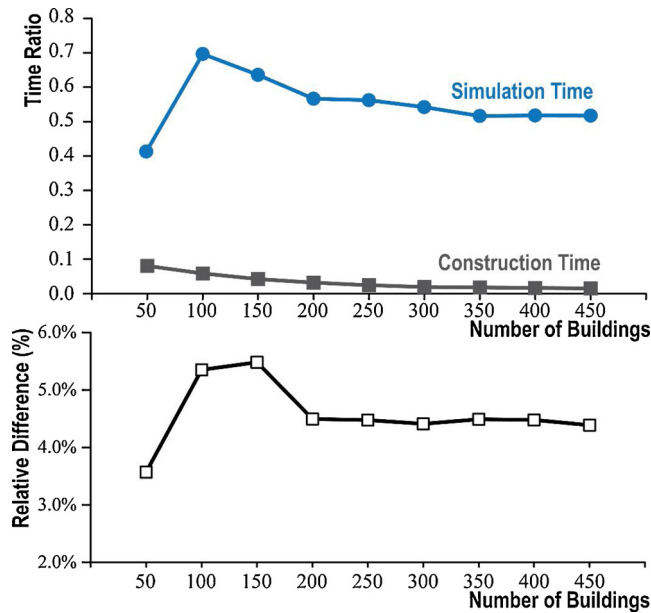**Fig. 5.** Sample buildings groups for validation test.

Fig. 6. The comparison results between LW-DAB model and the whole city model.

of the proposed method when compared with the conventional whole city model. Different from the LW-DAB model, the whole city model simulates the entire city model in a single model file and simultaneously computes the thermal environment for all buildings. As introduced in the previous section, the LW-DAB model decomposes the city model into a collection of building models. Therefore, in addition to the simulation time, the proposed model also has an extra step of construction. To compare both methods, the model running time and simulated whole city energy consumption were recorded for building groups with a different number of buildings (from 50 to 450 as shown in Fig. 5).

Fig. 6 shows the efficiency and accuracy of the LW-DAB model when compared with the conventional whole city simulation model. In the top figure in Fig. 6, the time ratio is computed by dividing the simulation time of the LW-DAB model with the whole city simulation time. As it can be seen that even if adding the construction time, the simulation time is shorter for LW-DAB model. Also, with the increase of the simulation scale, the ratio becomes smaller and converted to 0.5. The bottom figure in Fig. 6 suggests that the discrepancy of simulation

results between both models is small and acceptable (less than 5% after convergence).

4.2. Assessing UHI's impacts with local weather clusters

4.2.1. City dataset

The validation case utilized the open geographic dataset of the city of Portland, Oregon, USA (Bureau of Planning & Sustainability, 2019). The dataset includes the information of footprints and detailed building features of 1175 buildings. Fig. 7 shows the color-coded building footprints based on height and Fig. 8 is the constructed 3D city energy model. To simply the simulation the buildings' window-to-wall ratio (WWR) was set to 0.5 and all buildings used the same zone templates.

To determine the number of weather condition clusters, the LW-DAB model used h_{bld}, VH, and ρ_{bld} as the clustering coefficients. To compares the UHI's impacts of the localized climate conditions that the same city model was assumed to be located at three sites with different latitude, including

- Miami, Florida, USA (25°45'42.05" N, 80°11'30.44" W) - The city of Miami is the center of the state of Florida, USA. With a tropical monsoon climate, Miami has an average temperature of 28 °C in July and 20 °C in January.
- Hong Kong (22°17'7.87" N, 114°9'27.68" E) - Hong Kong is located on China's southern coast. Hong Kong has a humid subtropical climate and an average temperature of 29 °C in July and 16 °C in January.
- Singapore (1°17'24.97" N, 103°51'7.05" E) - Singapore is an island city-state in Southeast Asia. With a typical tropical climate,
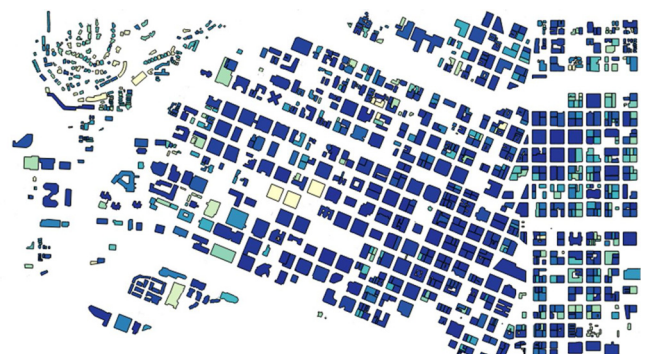

Fig. 7. Color-coded city footprint based on height.

Fig. 8. The 3D city building energy model.

Table 1
Classification coefficients for all culsters.

Cluster	Cluster 1	Cluster 2	Cluster 3	Cluster 4	Cluster 5
h_{bld}	26.243	41.305	47.444	174.070	88.744
VH	0.244	0.545	0.864	1.203	1.583
ρ_{bld}	0.137	0.262	0.385	0.300	0.432

Singapore has an average temperature of 27 °C in July and 26 °C in January.

4.2.2. Local weather clusters

To incorporate the impacts of UHI, LW-DAB utilized localized weather files for each building block. The LW generator applied a k-mean clustering algorithm to generate *k* weather clusters. With a cross-validation test based on the Akaike Information Criterion, 5 was determined as the most appropriate number of clusters. Table 1 summaries the coefficients of average building height (h_{bld}), vertical-to-horizontal urban area ratio (*VH*), and horizontal building density (ρ_{bld}) for all five clusters. The combination of these three coefficients determines how the weather files are assigned. Cluster 1, 2 and 3 mainly composes low-rise and sparse buildings that far from the city center, while Cluster 4 and 5 include high-rise and densely distributed buildings, which have large façade and highly populated buildings. As the clusters are determined by the classification coefficients rather than physical closeness, some buildings were assigned different local weather files even if they are close to each other, for example, some buildings of Cluster 4 and 5. Fig. 9 visualizes the UHI intensity of all clusters.

Fig. 10 compares the hourly dry-bulb temperature variations due to the UHI in each weather cluster. As it is seen that the UHI intensifies the temperature variation throughout the whole month. With the location weather generator, the urban cool island(UCI)phenomenon also observed as the variation sometimes is negative. The higher UHI intensity results in higher temperature variation from Cluster 1 to Cluster 5. However, the intensity's impact on local cluster temperature is mild in January in Miami.

Fig. 11 illustrates the daily average temperature variations in the whole year in Miami. The TMY weather in Miami in a year is relatively stable and seasonal differences are not obvious. In the figure, Cluster 5 shows the highest positive temperature variations. Although the highest
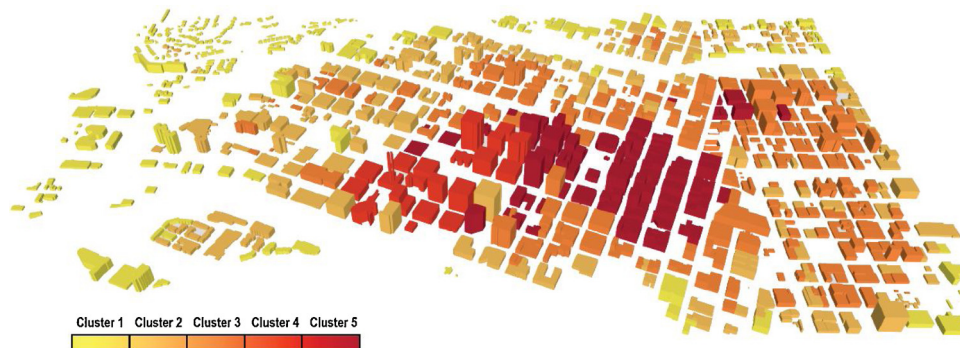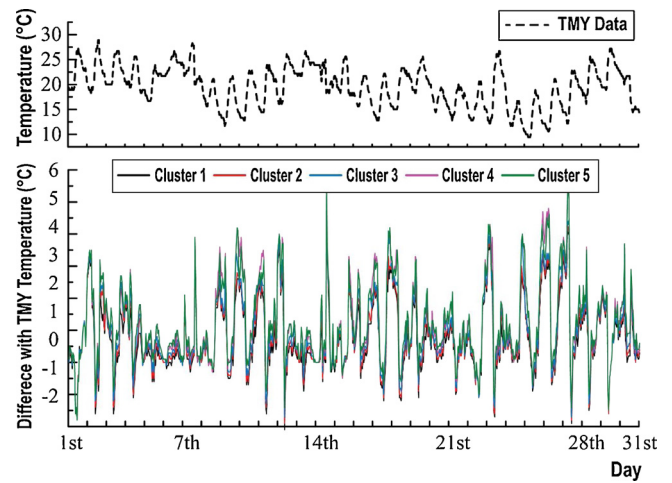

Fig. 10. The hourly dry bulb temperature and temperature variation generated by UHI clusters in Miami of TMY January.

temperature is shown at noon, the UHI's impact is not the highest. The temperature variation shows two peaks in the early morning after sunrise and later afternoon sunset. Comparing the temperature across the months, it can be seen that the yearly impacts of UHI are larger in the seasons that have relatively high or low temperatures, such as July and Jan. Also, all five clusters have a consistent trend due to the similar city weather condition. Also, from the generated temperature, it can be seen that Cluster 4 and Cluster 5 are similar to each other, except Mar, Apr, May, Jun, and Jul, although Table 1 suggests a higher difference between Cluster 4 (Higher average building height) and Cluster 5 (Higher horizontal building density). The possible reason is because of the proximity between Cluster 4 and Cluster 5. As shown in Fig. 9, although both clusters have distinctive morphological factors, part of clusters are close to each, which results in similar computational results from UWG. Therefore, it is suggested that a region-based division of clusters could be more suitable.

4.2.3. Impacts on the urban cooling demand

With the DAB algorithm, the energy dynamic of the 3D city model can be simulated. As this study mainly focuses on the tropical climate regions, the discussion mainly focuses on the simulated cooling load. To simplify the simulation, all buildings in the 3D city model used the residential building template. Fig. 12 summaries the increased cooling energy demand due to the UHI for all clusters in a different month. Cluster 5 has the highest increases over the year and reaches 18 % in July. Cluster 1 has the lowest increases within 2 %–10 %. Cluster 4 receives a similar impact as Cluster 5 in summer, but lower impacts in other seasons.
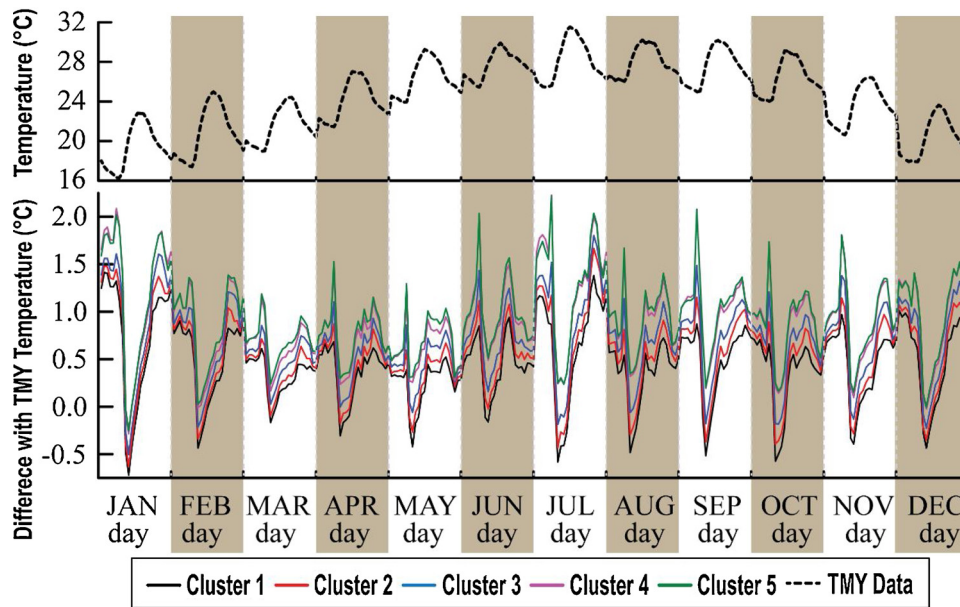

Fig. 9. Clustered UHI intensity of 3D city model.

Fig. 11. Average daily temperature and temperature variation of weather clusters in a year in Miami.

4.2.4. Comparison cross different climate regions

In this section, Figs. 13 and 14 compared the temperature variations of different clusters due to UHI in a winter and a summer month for all cities. It should be noted that the vertical axis shows the difference between the TMY temperature and the temperature generated with the LW-DAB algorithm in the same city not the temperature difference among cites. In Fig. 13, the temperature difference of Miami in winter is significantly greater than that of Hong Kong and Singapore, especially in the early morning before sunrise and late afternoon (around 5 pm). In addition, Miami has a slight UCI phenomenon at around 10 am. The trend in Hong Kong is similar to that of Singapore. Fig. 14 shows the impact of UHI in Hong Kong climate is smaller than that of Miami and Singapore. The simulation results of our model suggest that, with the same city morphology and building physics setting, the humid sub-tropical climate receives smaller impacts compared with the typical tropical and tropical monsoon climates. However, in the tropical monsoon climate, the heat island effect in winter is significantly higher than that in summer. In the climate region that has a large temperature difference between day and night, such as Singapore, the UHI's impact in summer can be magnified. This is the result of the heat absorption capacity of physical buildings. For example, when the outside temperature increases rapidly and exceeds the temperature of the walls, the

buildings begin to extract heat from the outside and store it, while the outside temperature decline quickly and lower than that of the walls, buildings will return the heat stored in the day to the surrounding environment, redistributing the heat in the building surface and the surrounding air. As the data resolution of the generated weather file is one-hour, large scale data comparison is difficult to read, therefore, Figs. 13 and 14 show a typical day in January (Jan 15) and July (Jun 15). More detailed information can refer to the Appendix.

4.2.5. Cooling demand increases in different climate regions

The LW-DAB model successively calculated the energy performance of corresponding buildings in Miami, Hong Kong, and Singapore. Fig. 15 shows the simulated cooling demand increases caused by the UHI in the three cities. For all clusters, the cooling load was increased to some degree and Singapore has the highest increase. Cluster 5 in Singapore has an increase of above 15 % for almost all months (the highest is 28 % in November). Hong Kong and Singapore have a higher increase in winter than in summer, while the cooling load increase reaches its maximum in summer for Miami. Then, the following conclusions can be drawn. First, the intensity of UHI is highly affected by the temperature difference between the day and night. After sunset, with the sudden drop in temperature the energy stored in the urban canyon during the
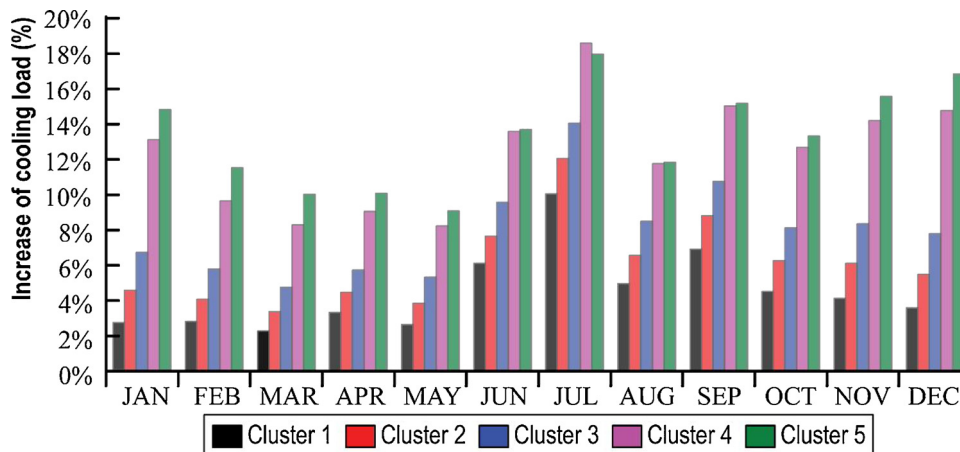

Fig. 12. The cooling load increases due to UHI for all clusters in the typical meteorological year.
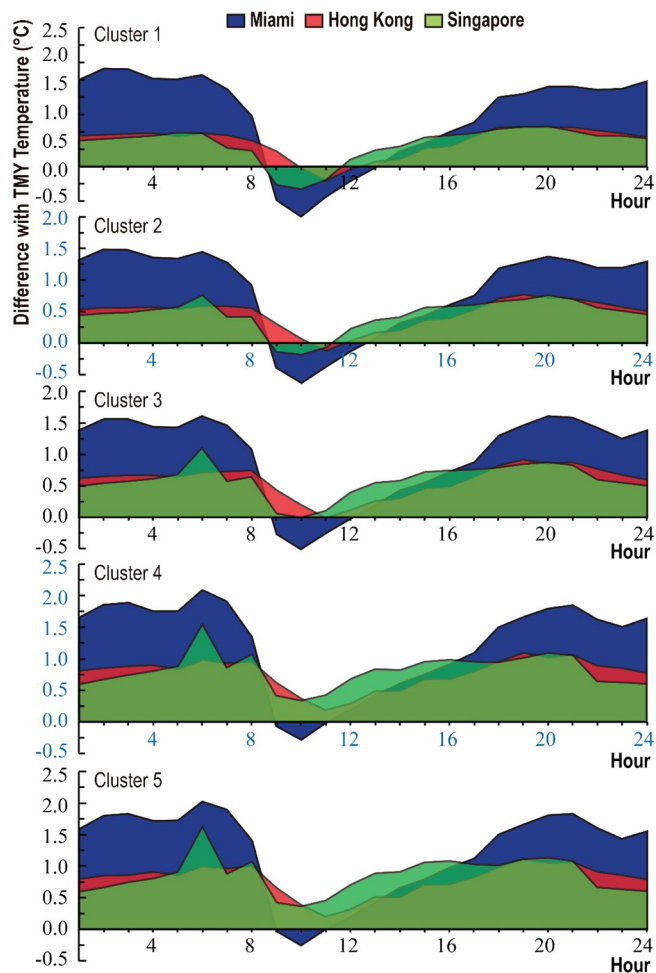
Fig. 13. The temperature variations in three cities in a typical day of January.

day is released into the surrounding environment, making the UHI effect more intensive. Second, the mild temperature variation does not necessarily mean the low cooling load increase.

5. Discussion

With the expansion of the growing cities, conventional simulation tools that apply the same weather assumption is not suitable for the entire city building environment. UHI is one of the causes of the variations of local microclimate in the dense urban region (Kämpf, 2009; Reinhart et al., 2013). Many researchers have proposed computational tools to assess the impacts of UHI and energy dynamics of urban buildings, such as CitySim (Robinson et al., 2009), UMI (Reinhart et al., 2013), and City Building Energy Saver (CityBES) (Chen et al., 2017). These tools can effectively assess city-scale building energy performance based on historical records and building physics. However, they are not suitable for large scale thermal dynamic simulation in the context of a huge number of buildings. To extend existing studies and develop a computationally efficient model for the simulation that incorporates UHI, this study proposed an LW-DAB model based on the concept of distributed modeling. By decomposing the whole city model into interrelated building units, the simulation allows flexible scale and variant climate conditions. According to the comparison results, the proposed method can half the total simulation time with less than 5% differences in simulation outcomes. The major simplification that allows such efficiency improvement is implementing IBEs to quantify the boundary conditions of the target building and its neighbor buildings and removing irrelevant components to save the computational
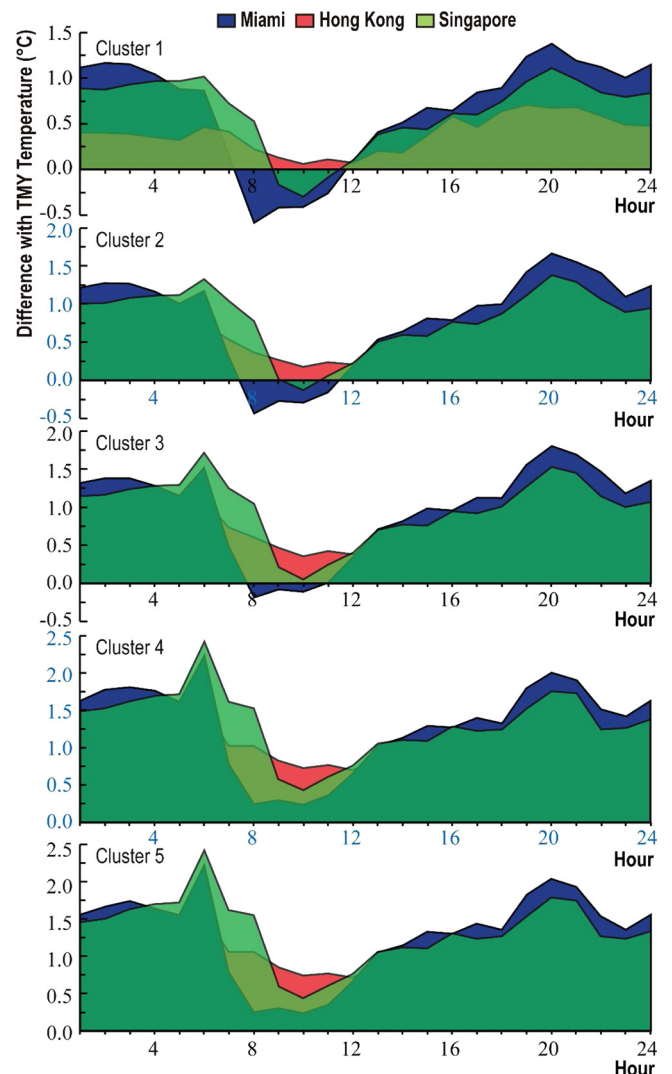

Fig. 14. The temperature variations in three cities in a typical day of July.

resources. As the boundary conditions and the local climate are customizable with refined local building information, the reliability of the proposed model also can be improved. In addition, the major bottleneck of large city-scale simulation is the limited computer running memory, which is often not sufficient to load the entire city model. The LW-DAB allows the computation tasks been assigned to multiple threads, processes, or servers without constraints of the model size.

The proposed local weather generator extended the UWG proposed by Bueno et al. (Bueno et al., 2013) through applying independent clustered weather generation and utilizing the aggregated solar path plane to modify the radiation level. By doing so, the LWG modifies the generic typical meteorological year of the geographic region and computes the variation based on a process that integrates the RSM, VDM, UBL, and UC-BEM models. The differences in the local temperature, humidity, and radiation can be implemented by the IBEs and reflected in the building energy load changes. It also can be seen from the validation experiment that when incorporating UHI's impact the cooling load can increase by 5%–25%. Investigating the distribution of UHI clusters in various climate regions can provide quantitative references on how UHI will affect the energy dynamics in urban buildings and help to improve the design and decision-making for urban planning. For example, the effects of avoiding condensed buildings or creating open areas, such as parks, can be quantified in terms of energy saving over the years. Also, the proposed LW-DAB model can be used for cross-city comparisons or longitudinal studies. As shown in the
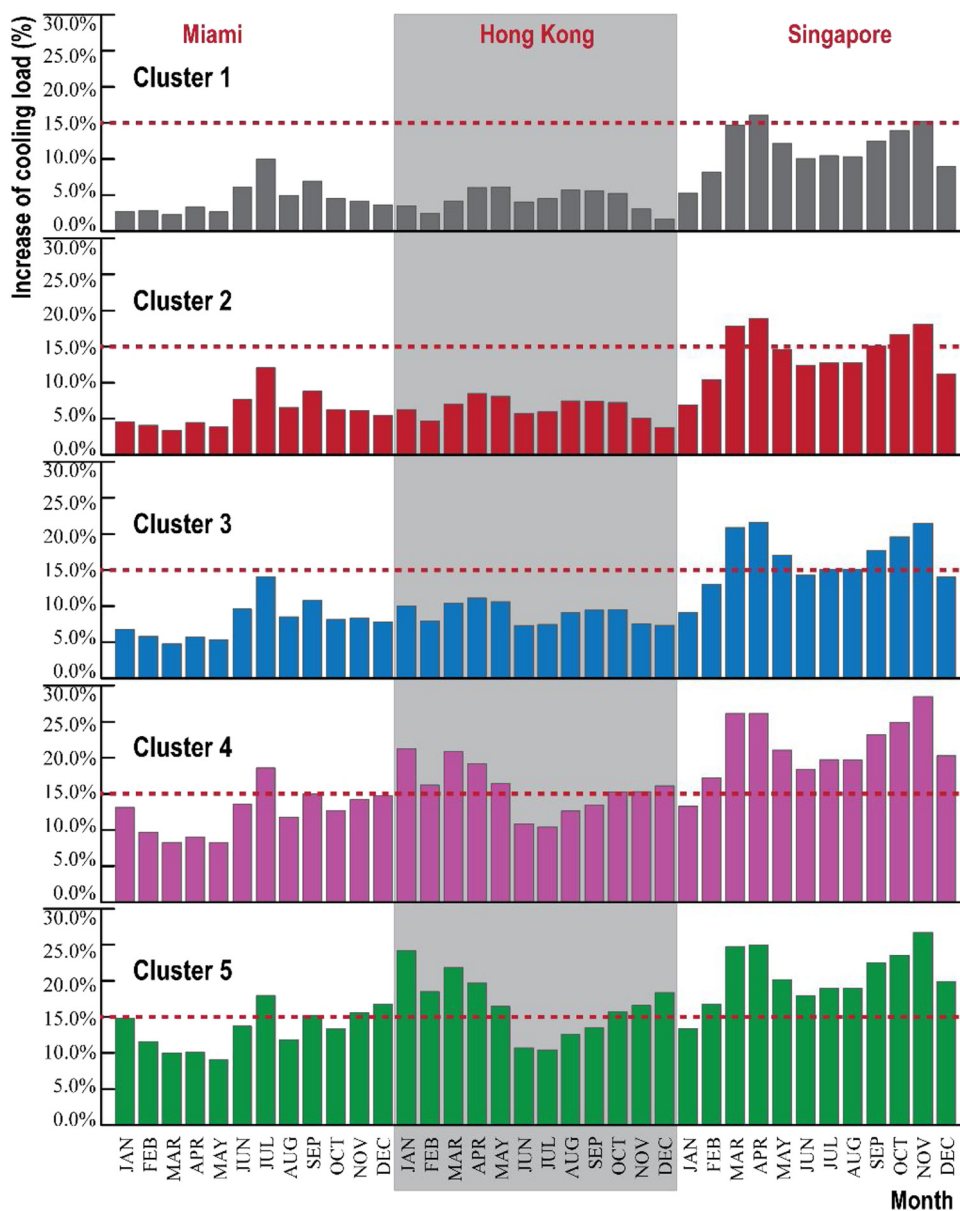
Fig. 15. Cooling demand increases for all three cities in a year.

comparison test of three cities' climate (Miami, Hong Kong, and Singapore), the UHI's impact over a year can be assessed. The proposed model enables researchers a powerful tool for the large-scale urban environment and resource analysis.

Although the proposed LW-DAB model has proven to be valid for the given city, it still subjects to several limitations. First, the weather clusters were computed only based on three fundamental urban morphological features, average building height (h_{bld}), vertical-to-horizontal urban area ratio (VH), and horizontal building density (ρ_{bld}). However, in practice, the UHI intensity is determined by more comprehensive variables, such as window-to-wall ratio, vegetation coverage, water coverage, the albedo and emissivity of roofs and walls, etc. It is suggested to develop a higher dimensional and detailed study on local weather clusterings for the urban buildings. Second, to simplify the validation case study, this study used the sample construction and thermal zone templates. In reality, each building is unique with different construction materials, structural designs, and occupancy profiles. Although this proposed model allows customizing individual buildings, due to the lack of resolution and information, this study is not able to apply unique zoning and construction configuration for each

building. Therefore, it is preferable to incorporate specific building information into the LW-DAB in the future. Third, the temperature variation in the study is the only consequence of UHI, however, UHI has more profound impacts on building environment, such as anthropogenic heat sources, radiative heat transfers, and air movements, can be extended in the future study.

6. Conclusions

With the rapid expansion in past decades, the buildings energy efficiency becomes crucial to the sustainable development of cities. Existing analysis and simulation tools for city energy dynamics are impeded its huge requirements of computational resources. To simplify the computation, these models have to omit the diversity of the local environment and reduce the model scale. This study developed an LW-DAB model that automatically assign localized weather conditions based on the intensity of UHI and distributed simulation through a decomposition and reaggregation process. The validation tests suggest that the proposed method is able to promote computational efficiency without sacrifying accuracy. The proposed model enables the

researchers and decision-makers an efficient tool to conduct large-scale studies of urban energy dynamics.

Declaration of Competing Interest

The authors declare that they have no known competing financial interests or personal relationships that could have appeared to influence the work reported in this paper.

References

Ali-Toudert, F., & Böttcher, S. (2018). Urban microclimate prediction prior to dynamic building energy modelling using the TEB model as embedded component in TRNSYS. *Theoretical and Applied Climatology, 134*(3–4), 1413–1428. https://doi.org/10.1007/s00704-018-2621-3.

Bueno, B., Norford, L., Hidalgo, J., & Pigeon, G. (2013). The urban weather generator. *Journal of Building Performance Simulation, 6*(4), 269–281. https://doi.org/10.1080/19401493.2012.718797.

Bureau of Planning and Sustainability (2019). *Building footprints - city of Portland.* Retrieved May 14, 2019, from PortlandMaps website:https://gis-pdx.opendata.arcgis.com/datasets/1078959662ce49cca059fe2f8930c194_48.

Chan, A. L. S. (2011). Developing a modified typical meteorological year weather file for Hong Kong taking into account the urban heat island effect. *Building and Environment, 46*(12), 2434–2441. https://doi.org/10.1016/j.buildenv.2011.04.038.

Chen, Y., Hong, T., & Piette, M. A. (2017). Automatic generation and simulation of urban building energy models based on city datasets for city-scale building retrofit analysis. *Applied Energy, 205*(August), 323–335. https://doi.org/10.1016/j.apenergy.2017.07.128.

Coakley, D., Raftery, P., & Keane, M. (2014). A review of methods to match building energy simulation models to measured data. *Renewable and Sustainable Energy Reviews, 37*, 123–141. https://doi.org/10.1016/j.rser.2014.05.007.

Coccolo, S., Kämpf, J., Mauree, D., & Scartezzini, J. (2018). Cooling potential of greening in the urban environment, a step further towards practice. *Sustainable Cities and Society, 38*(December 2017), 543–559. https://doi.org/10.1016/j.scs.2018.01.019.

Crawley, D. B. (2008). Estimating the impacts of climate change and urbanization on building performance. *Journal of Building Performance Simulation, 1*(2), 91–115. https://doi.org/10.1080/19401490802182079.

Dhalluin, A., & Bozonnet, E. (2015). Urban heat islands and sensitive building design – A study in some French cities' context. *Sustainable Cities and Society, 19*, 292–299. https://doi.org/10.1016/j.scs.2015.06.009.

Dogan, T., Reinhart, C., & Michalatos, P. (2016). Autozoner: An algorithm for automatic thermal zoning of buildings with unknown interior space definitions. *Journal of Building Performance Simulation, 9*(2), 176–189. https://doi.org/10.1080/19401493.2015.1006527.

Dorer, V., Allegrini, J., Orehounig, K., Moonen, P., Upadhyay, G., Kämpf, J., & Carmeliet, J. (2013). Modelling the urban microclimate and its impact on the energy demand of buildings and building clusters. *Proceedings of 13th Conference of the International Building Performance Simulation Association* (pp. 3483–3489).

Golany, G. S. (1996). Urban design morphology and thermal performance. *Atmospheric Environment, 30*(3), 455–465. https://doi.org/10.1016/1352-2310(95)00266-9.

Han, Y., Taylor, J. E., & Pisello, A. L. (2015). Toward mitigating urban heat island effects: Investigating the thermal-energy impact of bio-inspired retro-reflective building envelopes in dense urban settings. *Energy and Buildings, 102*, 380–389. https://doi.org/10.1016/j.enbuild.2015.05.040.

Han, Y., Taylor, J. E., & Pisello, A. L. (2017). Exploring mutual shading and mutual reflection inter-building effects on building energy performance. *Applied Energy, 185*, 1556–1564. https://doi.org/10.1016/j.apenergy.2015.10.170.

He, B.-J. (2019). Towards the next generation of green building for urban heat island mitigation: Zero UHI impact building. *Sustainable Cities and Society, 50*, 101647. https://doi.org/10.1016/j.scs.2019.101647.

He, J., Hoyano, A., & Asawa, T. (2009). A numerical simulation tool for predicting the impact of outdoor thermal environment on building energy performance. *Applied Energy, 86*(9), 1596–1605. https://doi.org/10.1016/j.apenergy.2008.12.034.

Ignatius, M., Wong, N. H., & Jusuf, S. K. (2015). Urban microclimate analysis with consideration of local ambient temperature, external heat gain, urban ventilation, and outdoor thermal comfort in the tropics. *Sustainable Cities and Society, 19*, 121–135. https://doi.org/10.1016/j.scs.2015.07.016.

Jin, H., Cui, P., Wong, N., & Ignatius, M. (2018). Assessing the effects of urban morphology parameters on microclimate in Singapore to control the urban heat island effect. *Sustainability, 10*(1), 206. https://doi.org/10.3390/su10010206.

Kämpf, J. J. H. (2009). *On the modelling and optimisation of urban energy fluxes, Vol. 4548*https://doi.org/10.5075/epfl-thesis-4548.

Kim, H., Gu, D., & Kim, H. Y. (2018). Effects of Urban Heat Island mitigation in various climate zones in the United States. *Sustainable Cities and Society, 41*, 841–852. https://doi.org/10.1016/j.scs.2018.06.021.

Kolokotroni, M., & Giridharan, R. (2008). Urban heat island intensity in London: An investigation of the impact of physical characteristics on changes in outdoor air temperature during summer. *Solar Energy, 82*(11), 986–998. https://doi.org/10.1016/j.solener.2008.05.004.

Kolokotroni, M., Giannitsaris, I., & Watkins, R. (2006). The effect of the London urban heat island on building summer cooling demand and night ventilation strategies. *Solar Energy, 80*(4), 383–392. https://doi.org/10.1016/j.solener.2005.03.010.

Ma, R., Geng, C., Yu, Z., Chen, J., & Luo, X. (2019). Modeling city-scale building energy dynamics through inter-connected distributed adjacency blocks. *Energy and Buildings, 202*, 109391. https://doi.org/10.1016/j.enbuild.2019.109391.

Macumber, D., Gruchalla, K., Brunhart-lupo, N., Gleason, M., Robertson, J., Polly, B., ... Schott, M. (2016). City scale modeling with openstudio. *2016 Building Performance Modeling Conference, (September), 133–140*.

Masson, V. (2000). A physically-based scheme for the urban energy budget in atmospheric models. *Boundary-layer Meteorology, 94*(3), 357–397. https://doi.org/10.1023/A:1002463829265.

Mauree, D., Naboni, E., Coccolo, S., Perera, A. T. D., Nik, V. M., & Scartezzini, J.-L. (2019). A review of assessment methods for the urban environment and its energy sustainability to guarantee climate adaptation of future cities. *Renewable and Sustainable Energy Reviews, 112*, 733–746. https://doi.org/10.1016/j.rser.2019.06.005.

Mauree, D., Blond, N., Kohler, M., & Clappier, A. (2017). *On the coherence in the boundary layer: Development of a canopy interface model, Vol. 4*, 1–12. https://doi.org/10.3389/feart.2016.00109 (January).

Mauree, D., Coccolo, S., Kaempf, J., & Scartezzini, J.-L. (2017). Multi-scale modelling to evaluate building energy consumption at the neighbourhood scale. *PLoS One, 12*(9), e0183437. https://doi.org/10.1371/journal.pone.0183437.

Mehaoued, K., & Lartigue, B. (2019). Influence of a reflective glass façade on surrounding microclimate and building cooling load: Case of an office building in Algiers. *Sustainable Cities and Society, 46*, 101443. https://doi.org/10.1016/j.scs.2019.101443.

Morini, E., Touchaei, A., Castellani, B., Rossi, F., & Cotana, F. (2016). The impact of albedo increase to mitigate the Urban Heat Island in Terni (Italy) using the WRF model. *Sustainability, 8*(10), 999. https://doi.org/10.3390/su8100999.

Oke, T. R. (1973). City size and the urban heat island. *Atmospheric Environment (1967), 7*(8), 769–779. https://doi.org/10.1016/0004-6981(73)90140-6.

Oke, T. R. (1982). The energetic basis of the urban heat island. *Quarterly Journal of the Royal Meteorological Society, 108*(455), 1–24. https://doi.org/10.1002/qj.49710845502.

Oke, T. R. (2006). Towards better scientific communication in urban climate. *Theoretical and Applied Climatology, 84*(1–3), 179–190. https://doi.org/10.1007/s00704-005-0153-0.

Peeters, L., De Dear, R., Hensen, J., & D'haeseleer, W. (2009). Thermal comfort in residential buildings: Comfort values and scales for building energy simulation. *Applied Energy, 86*(5), 772–780. https://doi.org/10.1016/j.apenergy.2008.07.011.

Perera, A. T. D., Coccolo, S., Scartezzini, J.-L., & Mauree, D. (2018). Quantifying the impact of urban climate by extending the boundaries of urban energy system modeling. *Applied Energy, 222*(December 2017), 847–860. https://doi.org/10.1016/j.apenergy.2018.04.004.

Pisello, A. L., Taylor, J. E., Xu, X., & Cotana, F. (2012). Inter-building effect: Simulating the impact of a network of buildings on the accuracy of building energy performance predictions. *Building and Environment, 58*, 37–45. https://doi.org/10.1016/j.buildenv.2012.06.017.

Pisello, A. L., Castaldo, V. L., Taylor, J. E., & Cotana, F. (2014). Expanding Inter-Building Effect modeling to examine primary energy for lighting. *Energy and Buildings, 76*, 513–523. https://doi.org/10.1016/j.enbuild.2014.02.081.

Reinhart, C. F., Dogan, T., Jakubiec, J. A. A., Rakha, T., & Sang, A. (2013). UMI – An Urban simulation environment for building energy use, daylighting and walkability. *The 13th Conference of International Building Performance Simulation Association, (January), 476–483*.

Robinson, D., Haldi, F., Leroux, P., Perez, D., Rasheed, A., & Wilke, U. (2009). CitySim: Comprehensive micro-simulation of resource flows for sustainable urban planning. *Proceedings of the Eleventh International IBPSA Conference* (pp. 1083–1090).

Salvati, A., Coch Roura, H., & Cecere, C. (2017). Assessing the urban heat island and its energy impact on residential buildings in Mediterranean climate: Barcelona case study. *Energy and Buildings, 146*(September 2018), 38–54. https://doi.org/10.1016/j.enbuild.2017.04.025.

Silva, J. S., da Silva, R. M., & Santos, C. A. G. (2018). Spatiotemporal impact of land use/land cover changes on urban heat islands: A case study of Paço do Lumiar, Brazil. *Building and Environment, 136*, 279–292. https://doi.org/10.1016/j.buildenv.2018.03.041.

Stewart, I. D., & Oke, T. R. (2012). Local climate zones for urban temperature studies. *Bulletin of the American Meteorological Society, 93*(12), 1879–1900. https://doi.org/10.1175/BAMS-D-11-00019.1.

Street, M., Reinhart, C., Norford, L., & Ochsendorf, J. (2013). Urban heat island in Boston–An evaluation of urban air-temperature models for predicting building energy use. *Proceedings of BS2013: 13th Conference of International Building Performance Simulation Association, 1022–1029*.

Swan, L. G., & Ugursal, V. I. (2009). Modeling of end-use energy consumption in the residential sector: A review of modeling techniques. *Renewable and Sustainable Energy Reviews, 13*(8), 1819–1835. https://doi.org/10.1016/j.rser.2008.09.033.

Torabi Moghadam, S., Coccolo, S., Mutani, G., Lombardi, P., Scartezzini, J.-L., & Mauree, D. (2019). A new clustering and visualization method to evaluate urban heat energy planning scenarios. *Cities, 88*, 19–36. https://doi.org/10.1016/j.cities.2018.12.007.

Touchaei, A. G., & Akbari, H. (2015). Evaluation of the seasonal effect of increasing albedo on urban climate and energy consumption of buildings in Montreal. *Urban Climate, 14*, 278–289. https://doi.org/10.1016/j.uclim.2015.09.007.

Wang, W., Chen, J., Hong, T., & Zhu, N. (2018). Occupancy prediction through Markov based feedback recurrent neural network (M-FRNN) algorithm with WiFi probe technology. *Building and Environment, 138*, 160–170. https://doi.org/10.1016/J.BUILDENV.2018.04.034.

Wang, W., Hong, T., Li, N., Wang, R. Q., & Chen, J. (2019). Linking energy-cyber-physical systems with occupancy prediction and interpretation through WiFi probe-based

ensemble classification. *Applied Energy, 236*, 55–69. https://doi.org/10.1016/J.
APENERGY.2018.11.079.

Xu, Y., Ren, C., Ma, P., Ho, J., Wang, W., Lau, K. K.-L., ... Ng, E. (2017). Urban mor-
phology detection and computation for urban climate research. *Landscape and Urban
Planning, 167*, 212–224. https://doi.org/10.1016/j.landurbplan.2017.06.018.

Xu, D., Zhou, D., Wang, Y., Xu, W., & Yang, Y. (2019). Field measurement study on the
impacts of urban spatial indicators on urban climate in a Chinese basin and static-
wind city. *Building and Environment, 147*, 482–494. https://doi.org/10.1016/j.
buildenv.2018.10.042.

Yang, X., Jin, T., Yao, L., Zhu, C., & Peng, L. L. (2017). Assessing the impact of urban heat
island effect on building cooling load based on the local climate zone scheme.
Procedia Engineering, 205, 2839–2846. https://doi.org/10.1016/j.proeng.2017.09.
904.

Zheng, Z., Chen, J., & Luo, X. (2019). Parallel computational building-chain model for
rapid urban-scale energy simulation. *Energy and Buildings, 201*, 37–52. https://doi.
org/10.1016/j.enbuild.2019.07.034.